.

Case Studies in Wave-Current Interaction

James C. McWilliams

Department of Atmospheric & Oceanic Sciences

Institute of Geophysics & Planetary Physics

U.C.L.A.

with Ken Melville, Juan Restrepo, Peter Sullivan, & Yusuke Uchiyama

Do surface waves matter to oceanic currents?

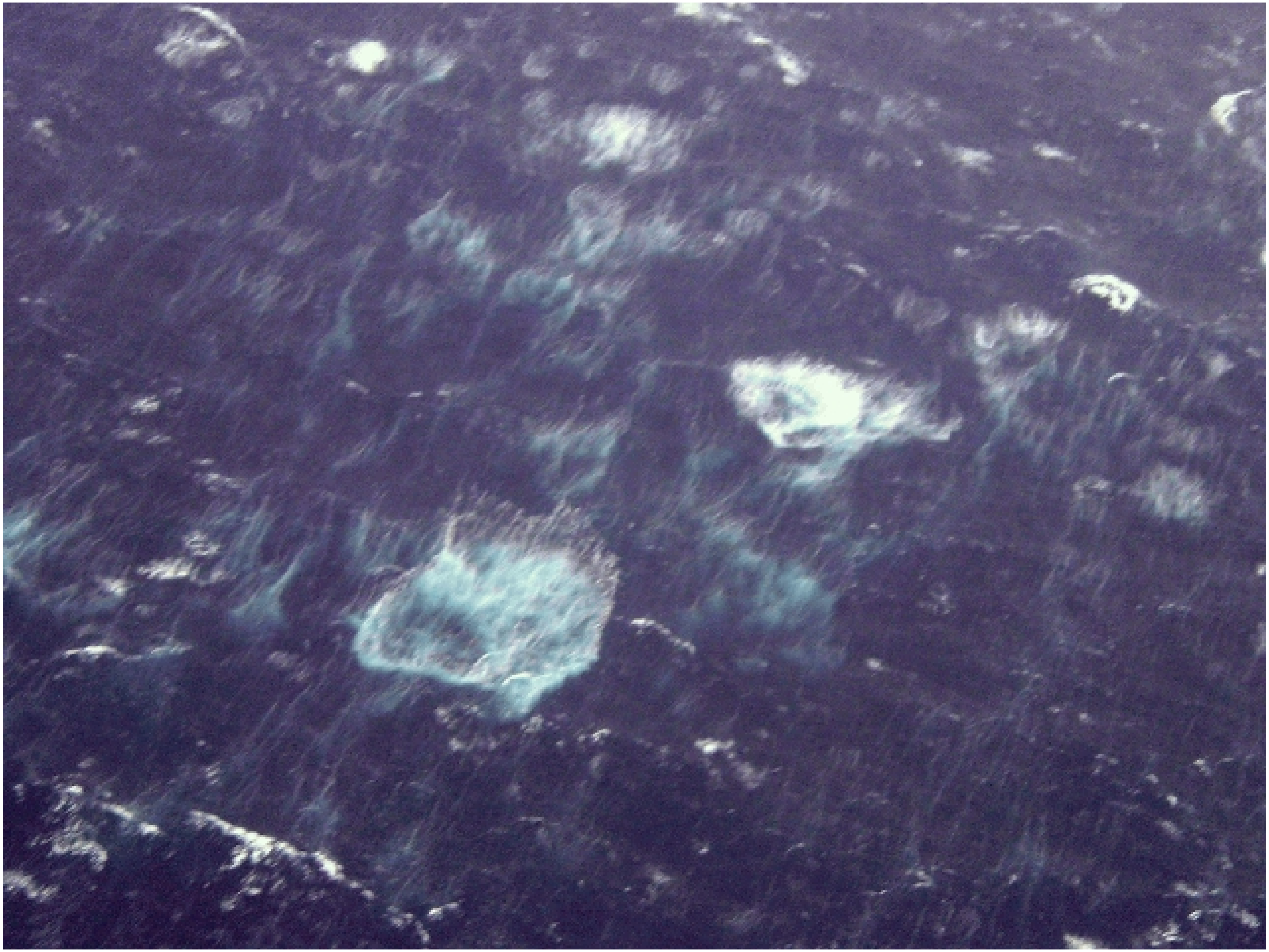

Aircraft photograph of the oceanic surface under a hurricane: $\zeta \sim 10$ m.

Famous Wave - Current Interaction Phenomena

- Coastal infragravity waves due to wave - wave nonlinearity (Longuet-Higgins, 1950; . . .)

- Littoral currents due to surf-zone wave breaking (Longuet-Higgins, 1970; . . .)

- Langmuir circulations due to wave-averaged vortex force (Craik & Leibovich, 1976; . . .)

Goal: To bring these and other wave-induced phenomena into ROMS (including as a non-hydrostatic Large-Eddy Simulation model; Kanarska *et al.*, 2007).

Theory of Wave Effects on Currents (WEC)

Taking advantage of temporal and horizontal scale separations & weak nonlinearity for spectrum-peak waves . . .

Elements:

- primary waves: $\zeta \sim a_o$, $L \sim 1/k_o$, $c_o = \omega_o/k_o \sim \sqrt{g/k_0 \sinh[k_o H]}$, $u \sim \epsilon c_o$; $\quad (\epsilon \equiv a_o k_o \ll 1;\ \mu \equiv kH \sim 1.)$
- wave-forced long waves and sea-level set-up: $\zeta \sim \epsilon a_o$, $L \sim 1/\epsilon^2 k_o$, $\omega \sim \epsilon^2 \omega_o$, $u \sim \epsilon^2 c_o$.
- wave-influenced currents in a rotating, stratified fluid: $\zeta \sim \epsilon a_o$, $L \gtrsim 1/k_o$, $\omega \sim \epsilon^4 \omega_o$ & Ω_e, $u \sim \epsilon^2 c_o$.

$\Longrightarrow$ multi-scale, primary-wave-averaged theory for WEC (McWilliams *et al.*, 2004; Lane *et al.*, 2007). Important quantities are the Lagrangian-mean horizontal current, Stokes drift, and quasi-static set-up:

$$\mathbf{v}_\perp^{St} = \overline{[\,(\int^t \mathbf{u}^{wave}\,dt')\cdot\boldsymbol{\nabla}\,]\,\mathbf{u}^{wave}} \quad \& \quad g\,\zeta^{set-up} = \overline{\left(\frac{\partial \zeta^{wave}}{\partial t}\right)^2} - \frac{\overline{(\mathbf{u}^{wave})^2}}{2} \le 0\,.$$

$$
\begin{aligned}
\frac{D\mathbf{u}}{Dt} + 2\boldsymbol{\Omega}_e \times \mathbf{u} + \frac{1}{\rho_o}\boldsymbol{\nabla} p + \frac{g\rho}{\rho_o}\hat{\mathbf{z}} + \mathcal{SGS} &= -\ \boldsymbol{\nabla}\mathcal{B} + \boldsymbol{\mathcal{V}} + \mathbf{B} \\
\boldsymbol{\nabla}\cdot\mathbf{u} &= 0 \\
\frac{D}{Dt}(\rho, C) + \mathcal{SGS} &= -\ \mathbf{u}^{St}\cdot\boldsymbol{\nabla}(\rho, C)
\end{aligned}
$$

with subgrid-scale parameterizations $\mathcal{SGS}$ and wave-averaged forcing terms,

- Bernoulli head: $\mathcal{B} \;=\; \frac{1}{2}\overline{(\mathbf{u}^{wave})^2}$
- Coriolis and vortex force: $\boldsymbol{\mathcal{V}} \;=\; \mathbf{u}^{St}\times(2\boldsymbol{\Omega}_e + \boldsymbol{\nabla}\times\mathbf{u})$
- pseudo-3D Stokes advection: $\mathbf{u}^{St} \;=\; (\ \mathbf{v}_\perp^{St},\ \ -\boldsymbol{\nabla}_\perp\cdot\int_{-H}^{z}\mathbf{v}_\perp^{St}\,dz'\ )$.
- Parameterized acceleration due to wave breaking: $\mathbf{B}$.

Surface boundary conditions at wave-averaged sea level ($z = \zeta$) are

$$
w(\zeta) - \frac{D\zeta}{Dt} \;=\; \boldsymbol{\nabla}_\perp\cdot\int_{-H}^{\zeta}\mathbf{v}_\perp^{St}\,dz, \qquad \frac{1}{\rho_o}\left(p(\zeta) + p^{atm}\right) - g\zeta \;\approx\; -\overline{\left(\frac{\partial\zeta^{wave}}{\partial t}\right)^2}\,.
$$

Infragravity Waves in the Deep Ocean: Generation by WEC, Propagation, and Seismic Hum Excitation

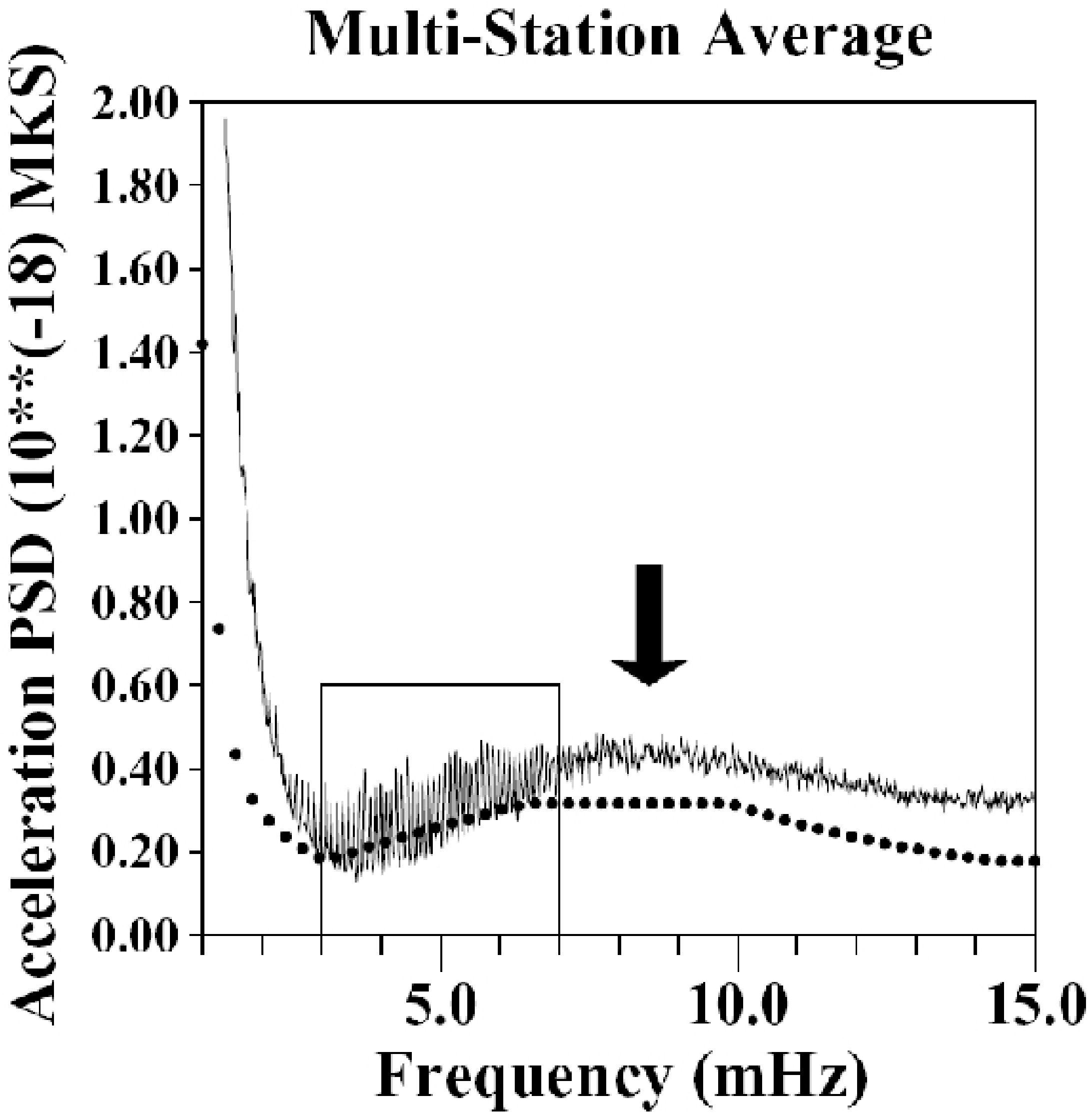

Composite frequency spectrum of global seismic acceleration (Tanimoto, 2005), compared to background noise (dots). Notice Earth's hum lines at 2-7 mHz (box) and a broad variance peak (arrow) in quiet periods without earthquakes. Are these caused by coastal and open-ocean infragravity waves? **Yes:** Rhie & Romanowicz (2005, 2006) and Webb (2007). **But how?**

Infragravity Wave Dyanmics

When the primary wave field changes over intervals of $10^2 - 10^4$ s and/or distances of $10 - 10^3$ km, the small-amplitude ($\sim$ mm) sea-level response is

$$\left[\frac{\partial^2}{\partial t^2} - \boldsymbol{\nabla} \cdot gH\boldsymbol{\nabla}\right] \zeta^{igw} \; = \; -\frac{\partial}{\partial t} \left[\boldsymbol{\nabla} \cdot \int_{-H}^{0} \mathbf{v}_{\perp}^{St} \, dz + \frac{\partial \zeta^{set-up}}{\partial t}\right] + \mathcal{SGS} \, .$$

The infragravity free-wave speed is $C \; = \; \sqrt{gH} \sim$ 20 m/s (shallow) – 200 m/s (deep).

.

.

The freely propagating modes are either *isotropic* in the open ocean or *edge-trapped* and propagating alongshore.

.

.

The forced components are either *bound* to a slowly varying forcing pattern (*e.g.*, a storm) or *propagating* (even resonant) for primary-wave forcing scales in the ranges above. The latter generate Earth's hum with bottom-pressure fluctuations, $g\rho_o\zeta^{igw}$.

.

.

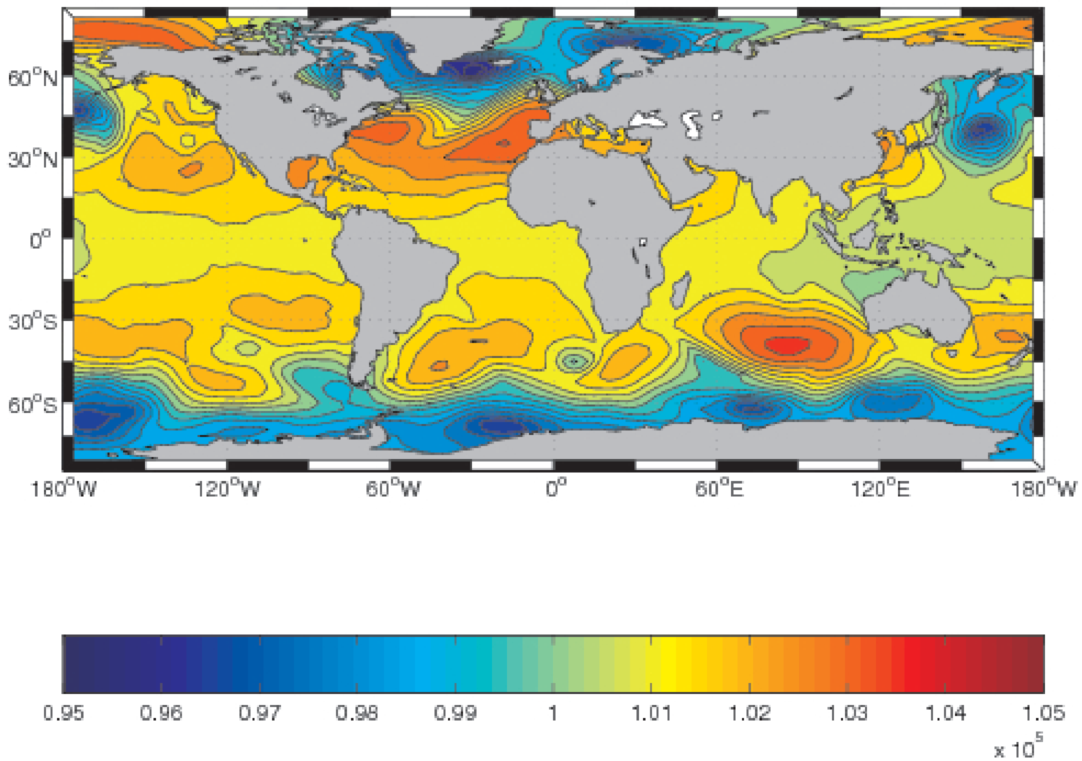

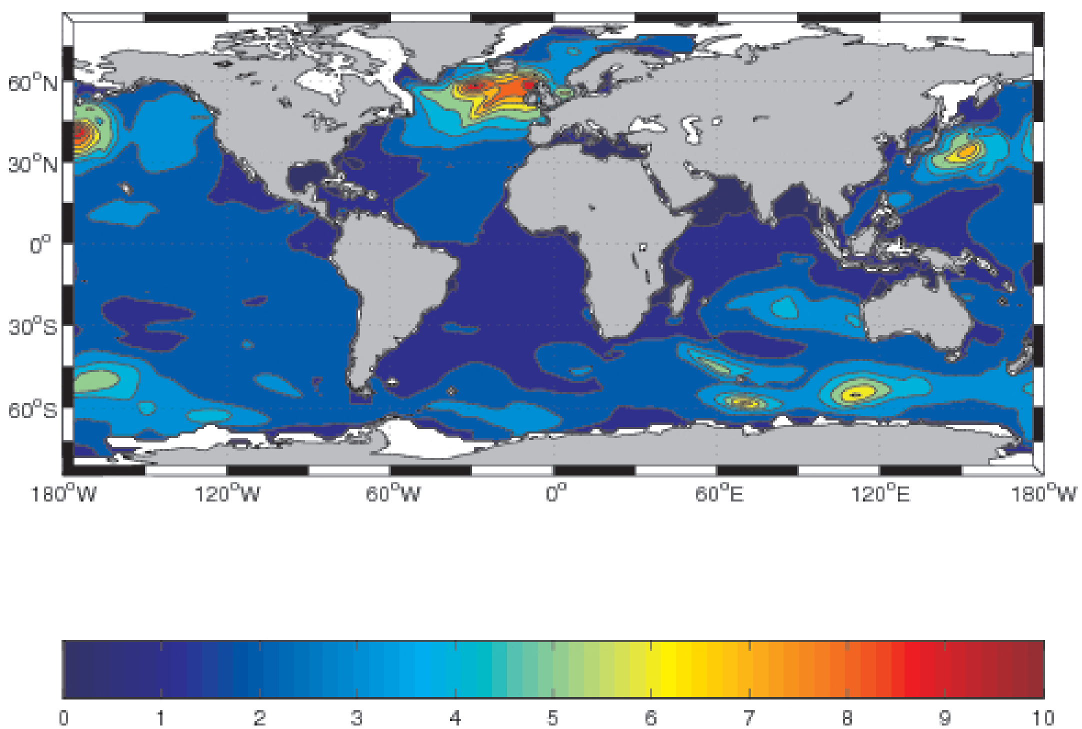

Operational Wave Analyses

European Center for Medium-range Weather Forecasts (ECMWF) analysis for 9 February 2000:
(**top**) sea-level pressure [Pa];
(**bottom**) primary wave height [m].

Notice the correspondence between strong cyclonic storms in the North Pacific and Atlantic and high wave heights.

The wave analysis is used to force the infragravity wave model.

Primary Wave Spectra

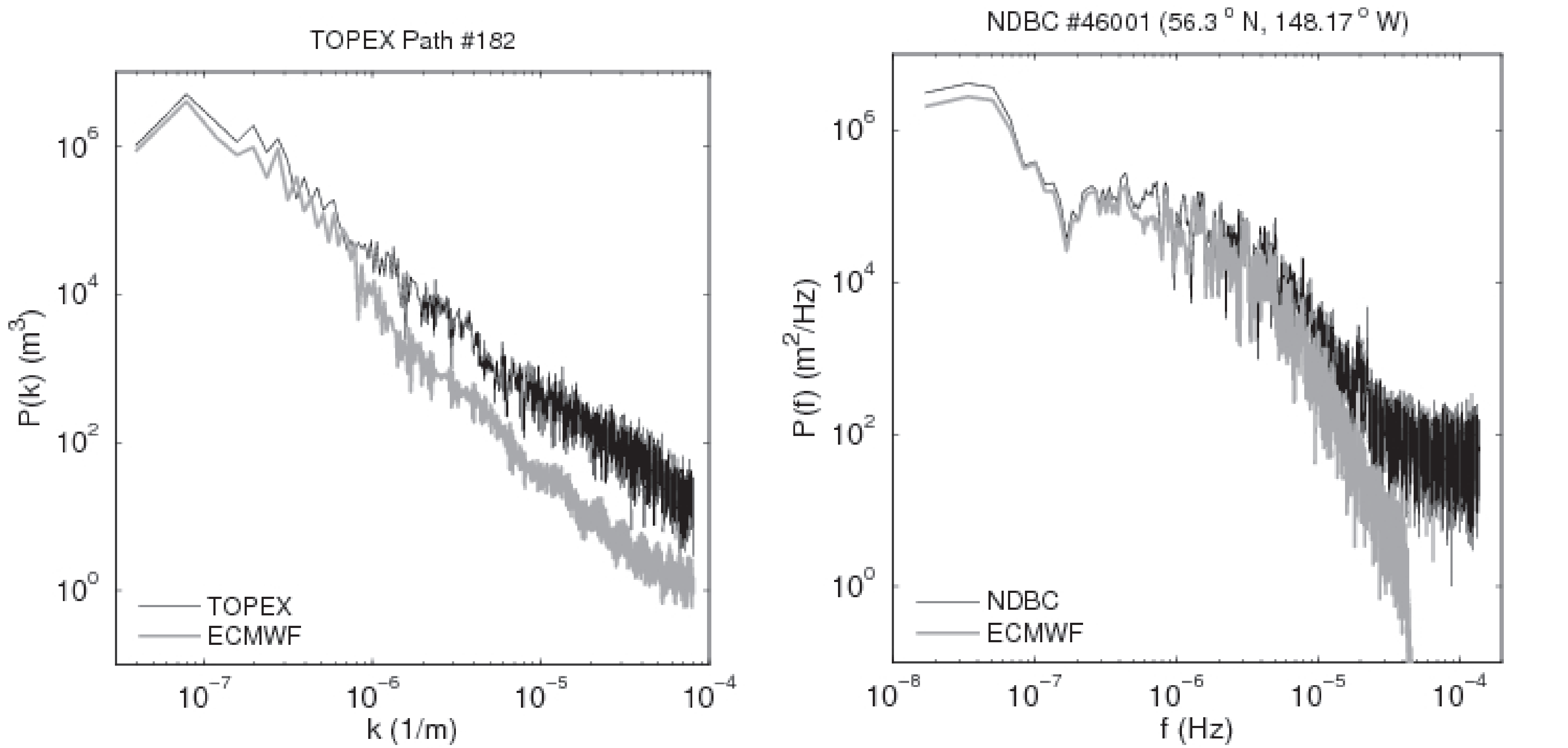

Black: TOPEX wavenumber spectra (right; eastern Pacific) and NDBC frequency spectra (left; near Alaska) of significant wave height.

Gray: ECMWF wave analyses linearly interpolated for the same time and place.

Notice the mesoscale primary-wave field variability. This is incorporated in the infragravity wave forcing either by random-phase spectrum extrapolation or by regional simulations with the SWAN model.

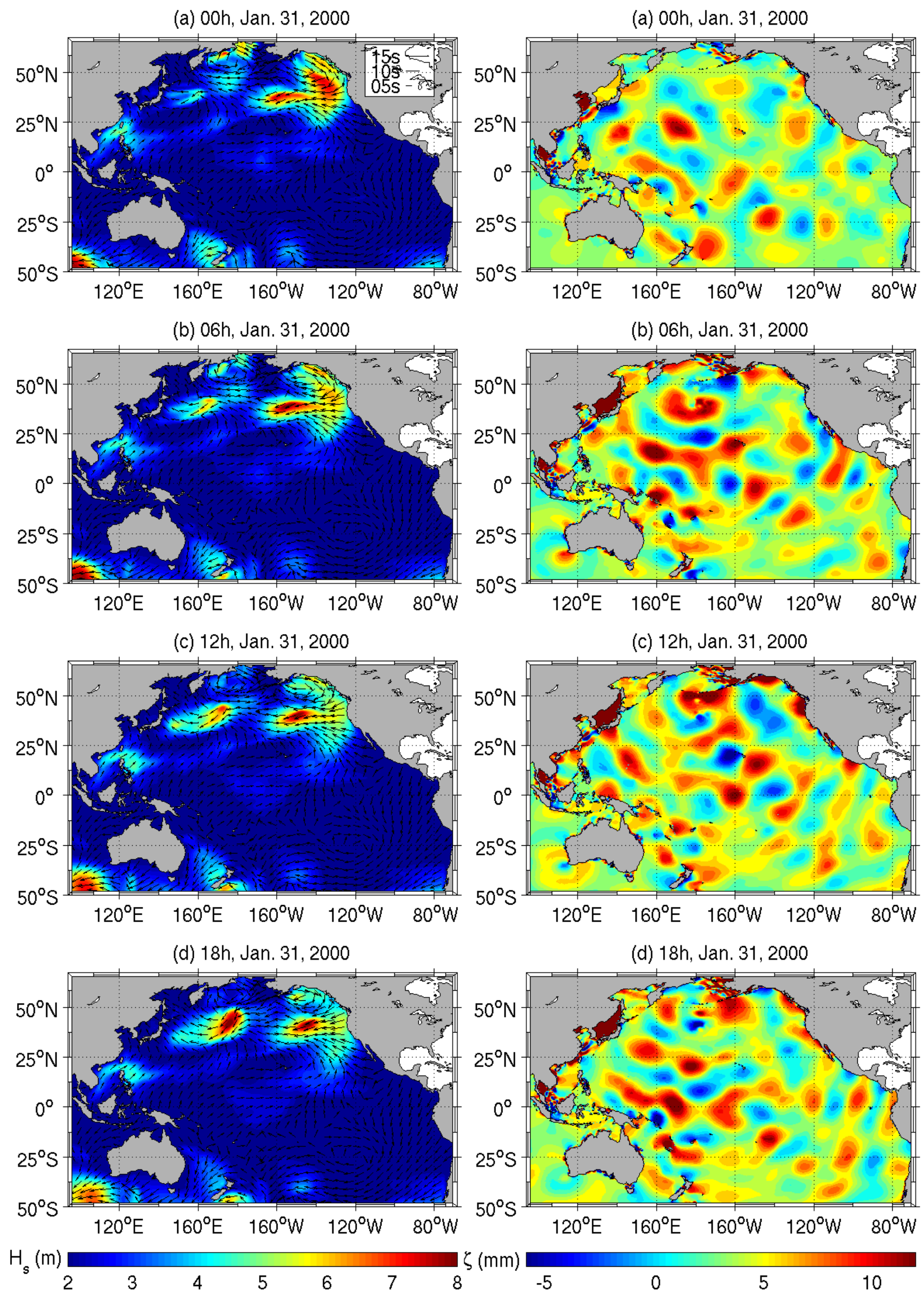

Results with ROMS:

Six-hourly snapshots in the Pacific Ocean: (left) the forcing (the significant wave height H_s [m] and mean wave direction), and (right) the ζ^{igw} response field [mm] on January 31, 2000.

- Freely propagating waves are ubiquitous over the basin and not simply correlated with the forcing.
- Leaky coastal generation of ζ^{igw} is comparable to open-ocean in deep water.
- Mesoscale primary wave variability strongly enhances the amplitude of ζ^{igw}.
- Simulated ζ^{igw} is sufficient to cause observed hum magnitudes and temporal variability.

(Uchiyama & McWilliams, 2007)

WEC and Shear Instability of a Littoral Current

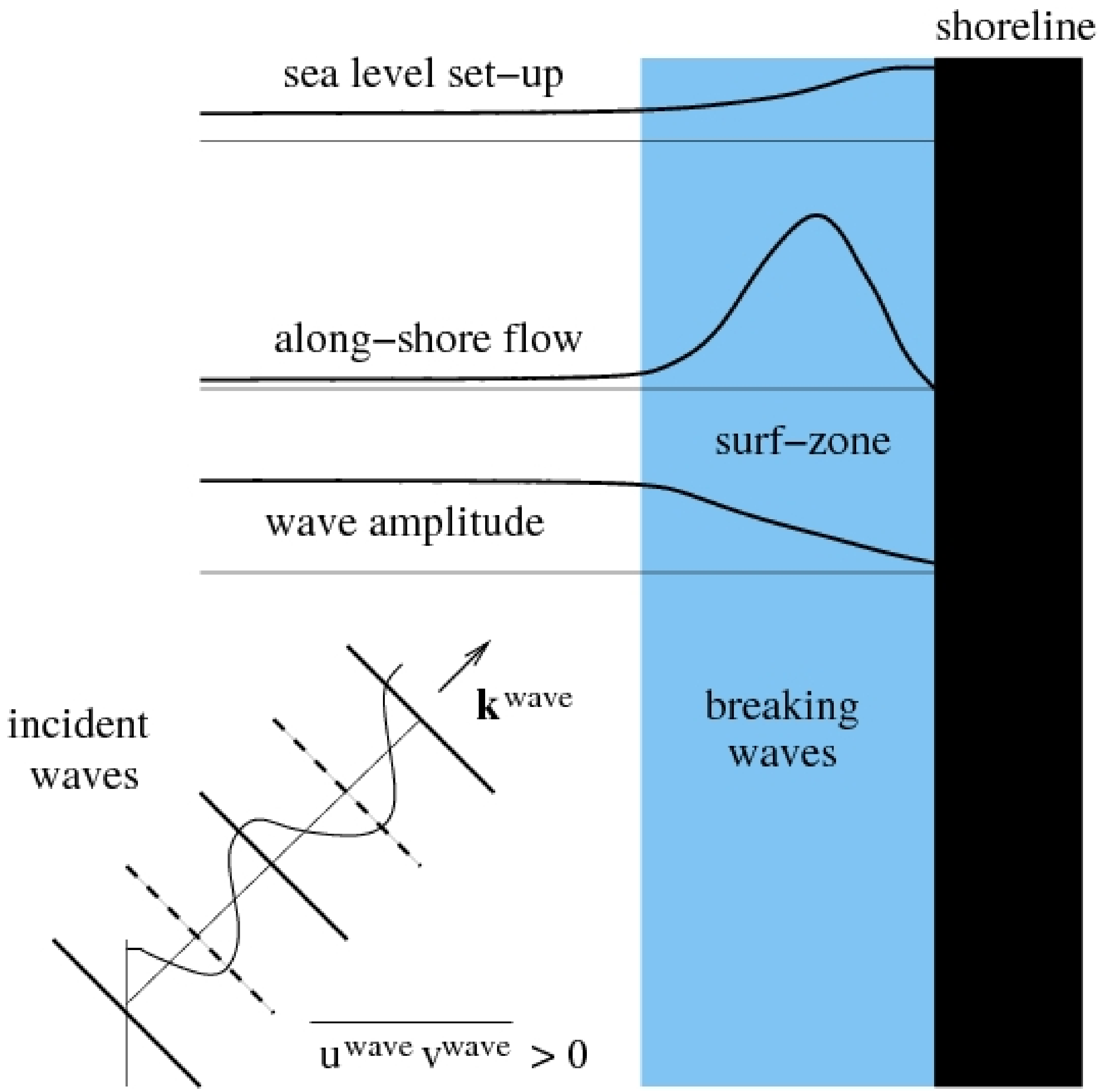

An alongshore littoral current and cross-shore sea-level set-up generated by surf-zone breaking of obliquely incident surface gravity waves (Longuet-Higgins, 1970). Further WEC effects arise with alongshore non-uniformity, *i.e.*, rip currents (Yu & Slinn, 2003).

Sometimes this current is observed to have a horizontal-shear instability, but almost all modeling studies thus far have not included WEC (Slinn *et al.*, 1998; Dodd *et al.*, 2000).

- Newburger & Allen (2007) is a brief exception.

Problem: An alongshore-uniform, barotropic current on a barred beach with incident, breaking waves and linear bottom drag, $\mathbf{D} = -r\mathbf{u}$. Compare cases with and without WEC and/or wave refraction by currents (CEW). Initial condition is the 1D steady, stable solution. For a case without WEC or CEW ($i.e.$, "zip"), the bottom drag acts to restore the alongshore flow to the mean flow with WEC+CEW.

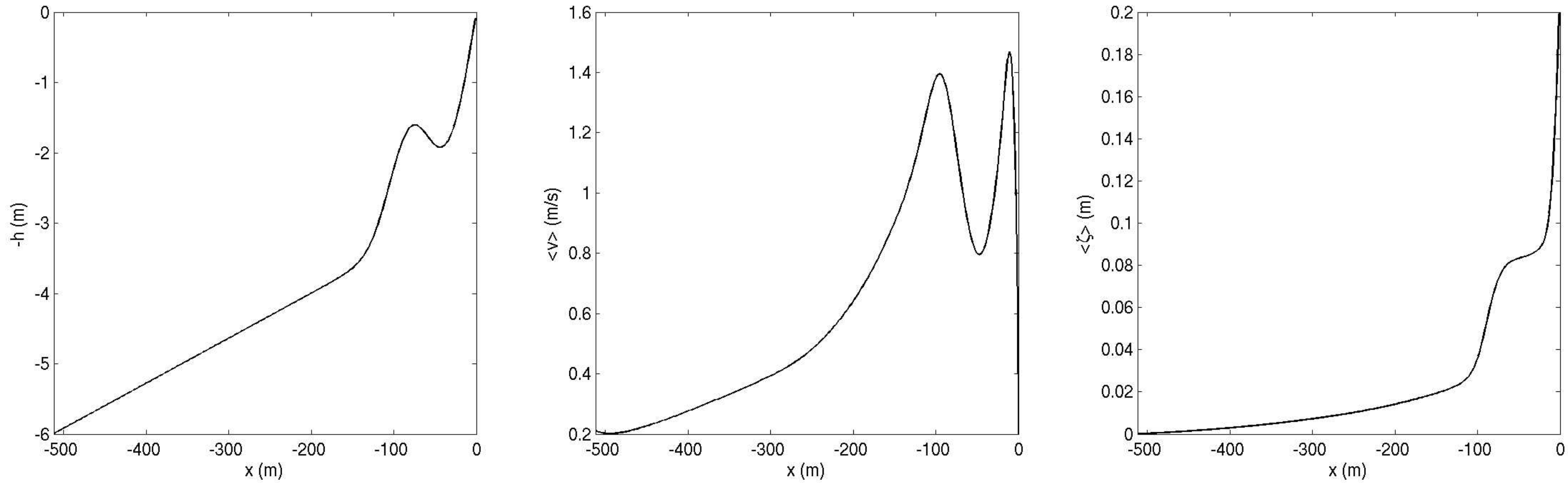

(Left) barred-beach topography $h(x)$, (center) mean alongshore current $\overline{v}(x)$, and (right) mean sea-level $\overline{\zeta}(x)$ (set-up) in an equilibrium, unstable case with WEC+CEW using ROMS.

(work in progress with Yusuke Uchiyama and Juan Restrepo)

Comparing Three Cases

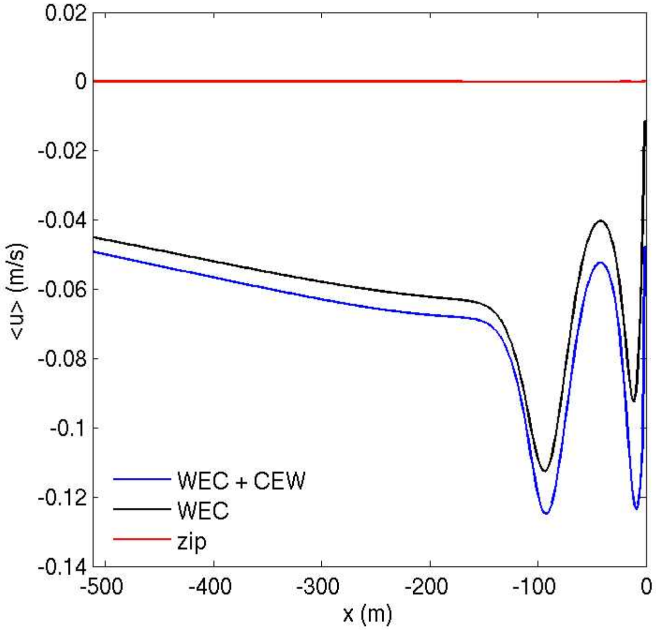

mean cross-shore current

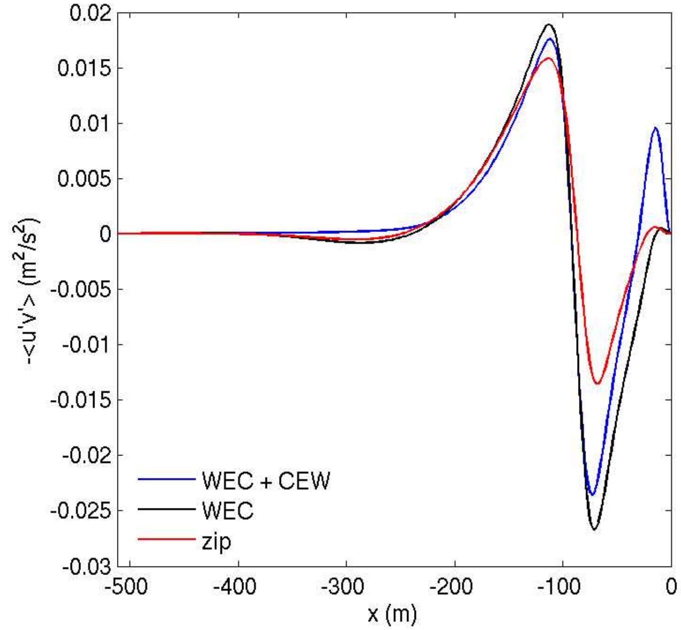

eddy Reynolds stress

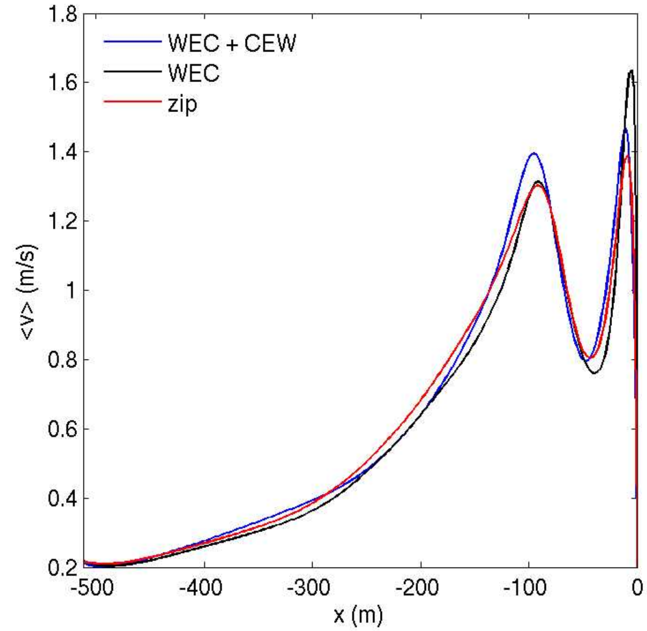

mean alongshore current

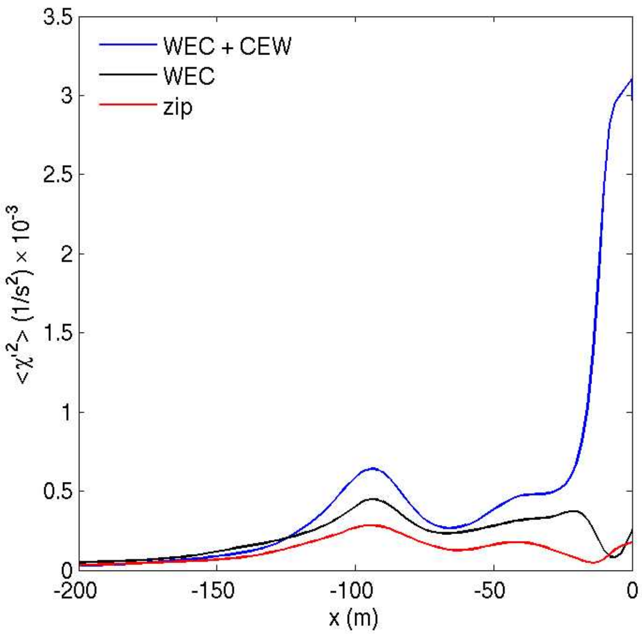

eddy enstropy

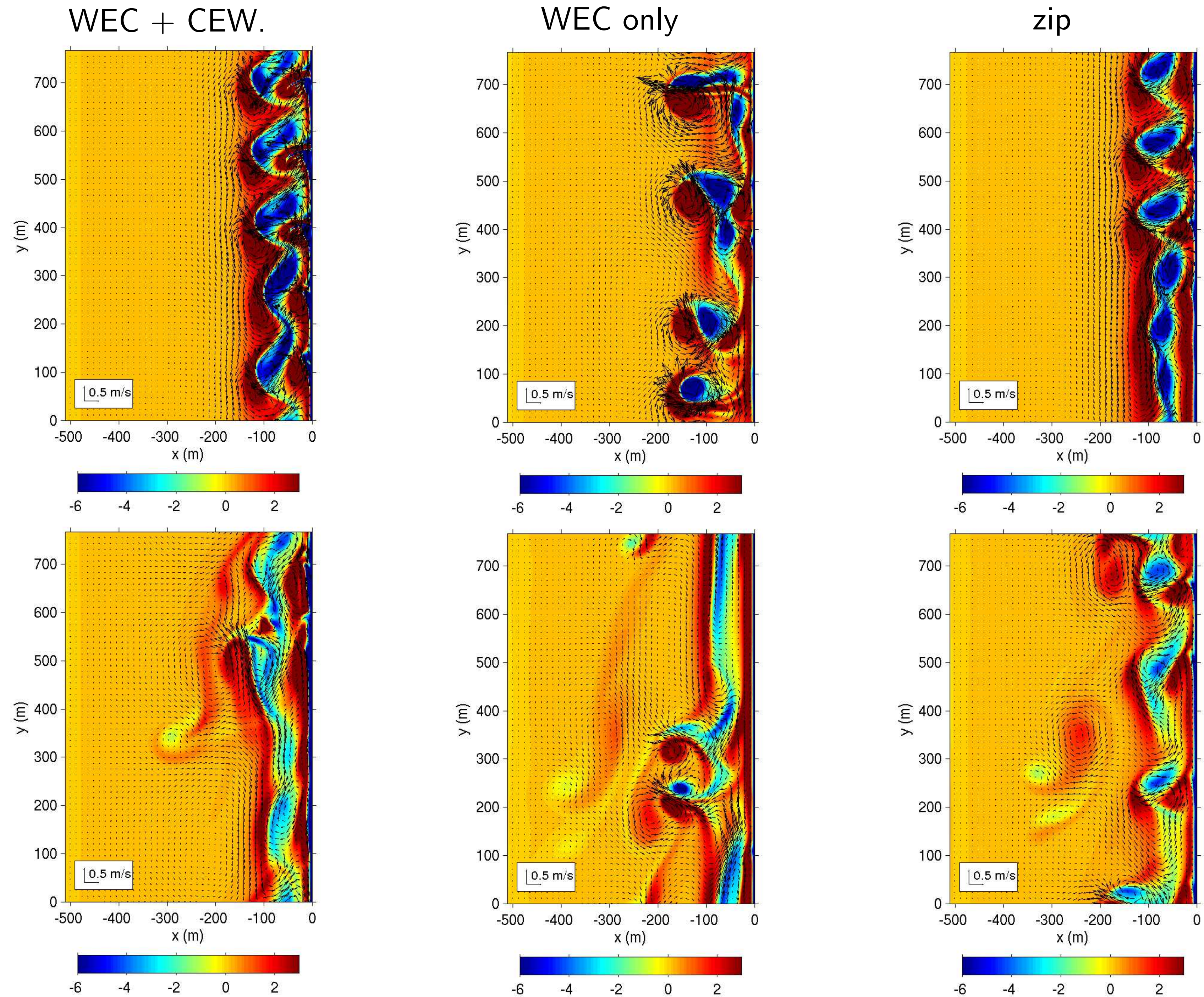

Vorticity χ $[10^{-3}s^{-1}]$ (color) and $\mathbf{u}$ (arrow) at $t = 15$ min (top row) and 6 hr (bottom)

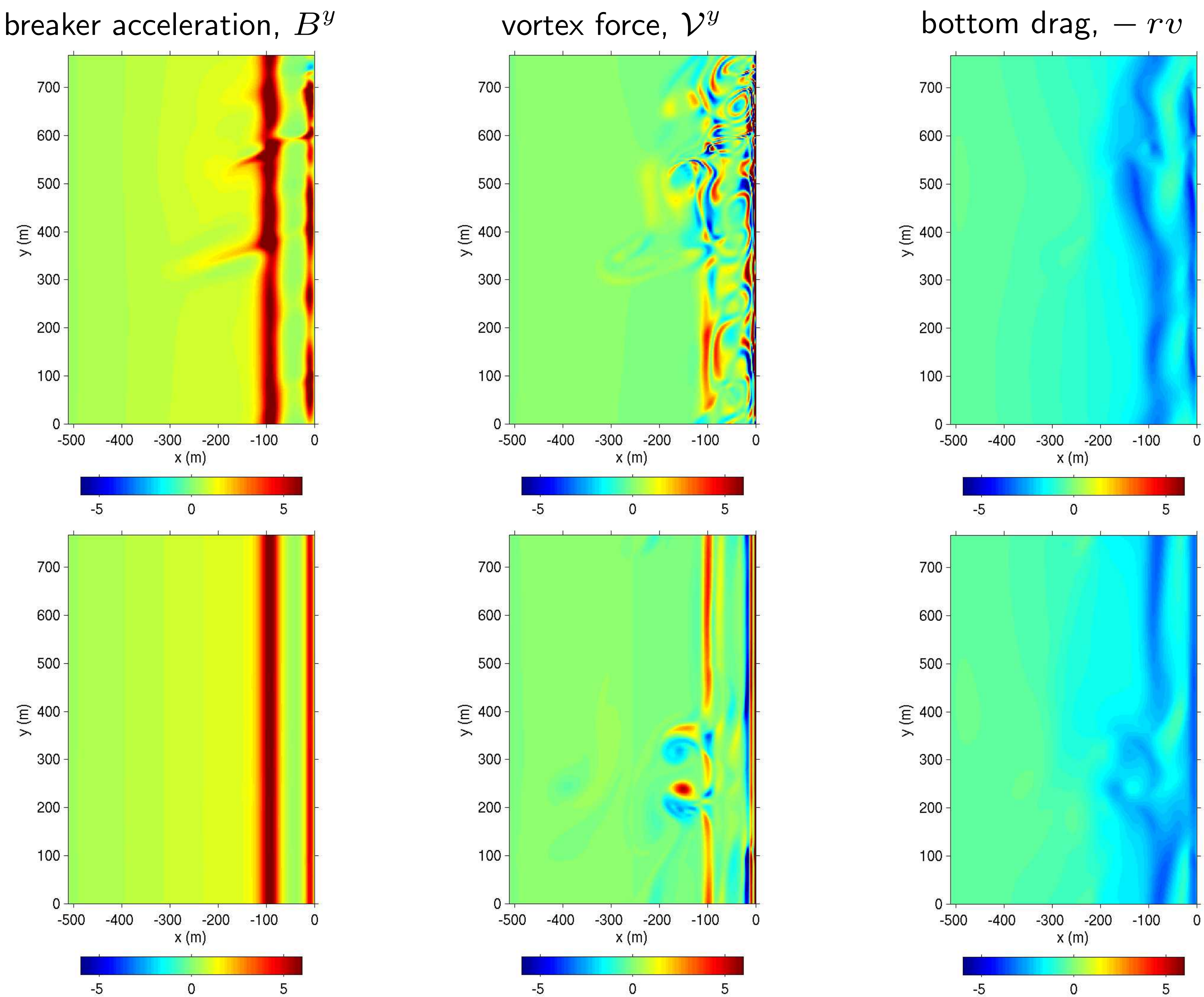

Alongshore forces $[10^{-3}\text{m s}^{-2}]$ at $t = 6$ hr for WEC+CEW (top row) and WEC only (bottom)

WEC in the Oceanic Boundary Layer: LES with Vortex Force and Stochastic Breakers

A single breaking wave provides a local, deterministic momentum impulse $\mathbf{B}(\mathbf{x}, t)$ on the scales resolved by a LES model plus a sub-grid-scale energy generation rate $W(\mathbf{x}, t) \sim \mathbf{c} \cdot \mathbf{B}$ in a volume spreading downward and forward from the onset point at the surface (:

$$\frac{\partial \mathbf{u}}{\partial t} = \cdots + \mathbf{B}, \quad \frac{\partial e}{\partial t} = \cdots + W \ ,$$

with e the SGS kinetic energy.

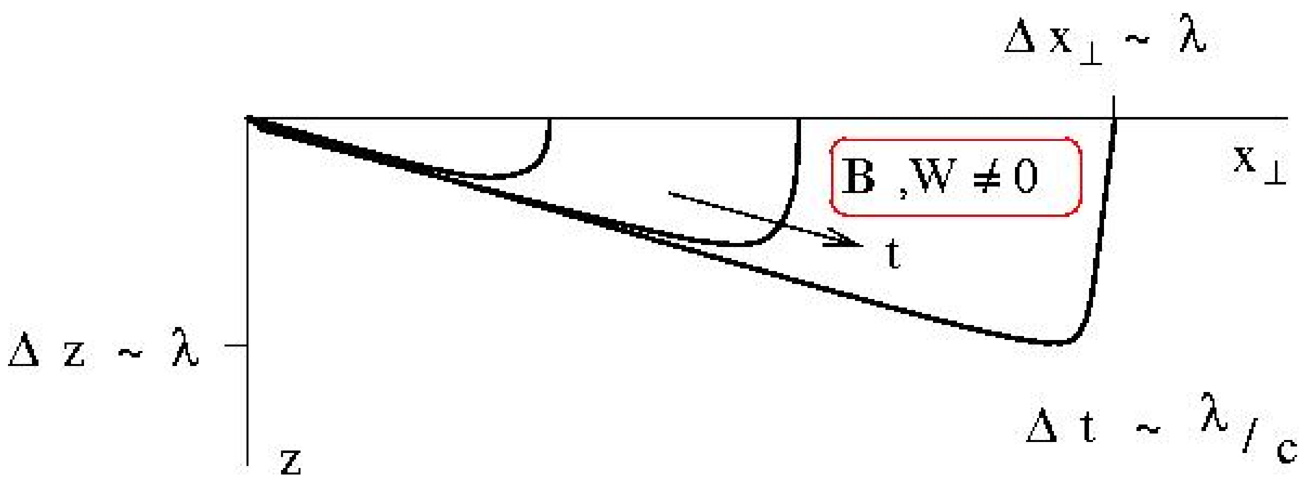

$\mathbf{B}$ & W depict the effect of a breaking event after the completion of the initial plunging and/or spilling motions (Melville *et al.*, 2002). Turbulence develops from a resolved-scale instability in the response to $\mathbf{B}$.

In a LES (not ROMS), $\mathbf{B}$ & W are the sum of discrete breaking events randomly located in $(\mathbf{x}, t)$ and randomly distributed in $\mathbf{c}$, each with a coherent local shape (Sullivan *et al.*, 2007). In wind-wave equilibrium, the mean surface stress and energy input to the ocean are

$$\frac{1}{\rho_o}\,\boldsymbol{\tau}^{atm} = N_b \int d\mathbf{c}\, P[\mathbf{c}] \int\int dt\, d\mathbf{x}\, \mathbf{B}[\mathbf{c}] \sim \left(U^{atm}\right)^2$$

$$\mathcal{E}^{atm} = N_b \int d\mathbf{c}\, P[\mathbf{c}] \int\int dt\, d\mathbf{x}\, (\mathbf{c}\mathbf{B}[\mathbf{c}] + W[\mathbf{c}]) \sim \left(U^{atm}\right)^3 .$$

N_b is the breaker number density and $P[\mathbf{c}]$ is its empirically determined PDF for primary wave speed $\mathbf{c}$ as a function of U^{atm} and wave age, $A = c_p/U^{atm}$.

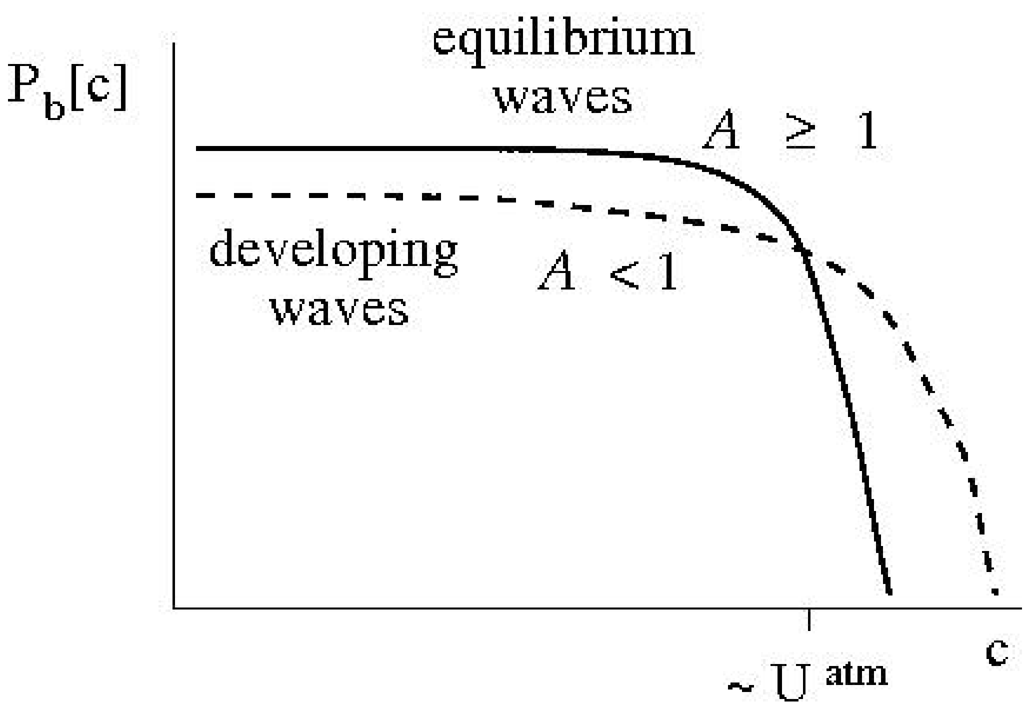

$\boldsymbol{\tau}^{atm}$ and $\mathcal{E}^{atm}$ are empirically determined from bulk formulae, as is the wave sea-level specturm used to calculate $\overline{v}_{\perp}^{St}(z)$.

Comparing Cases with and without Vortex Force and/or Breakers

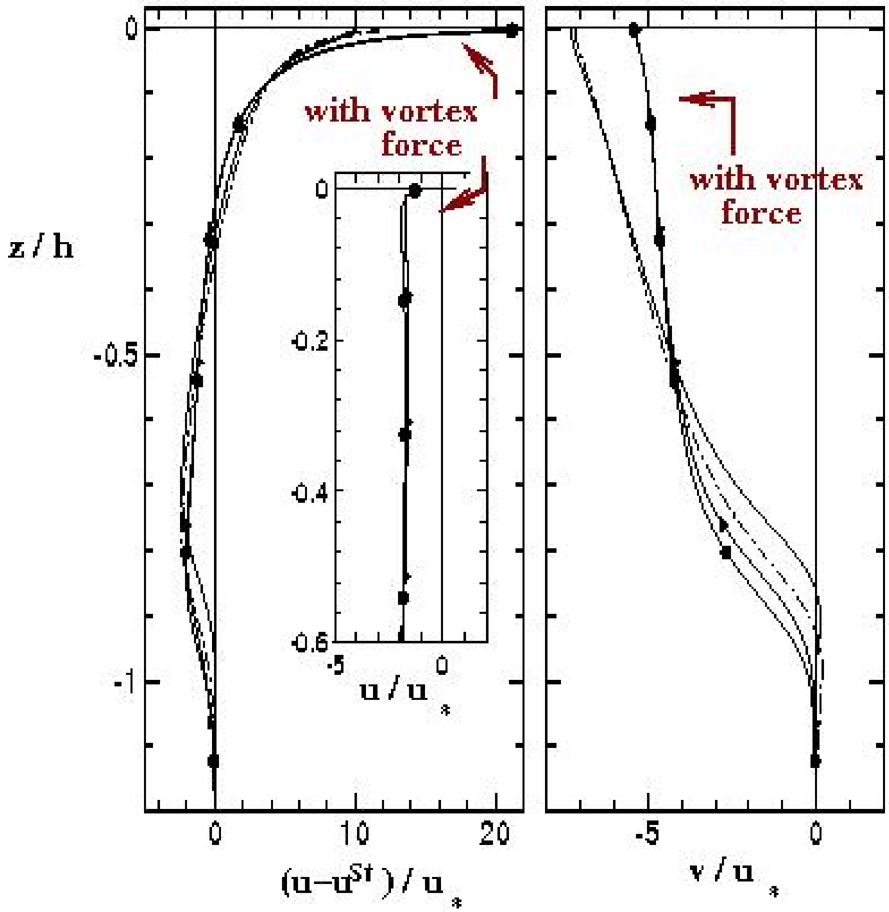

mean Ekman current,
depth-limited by stratification

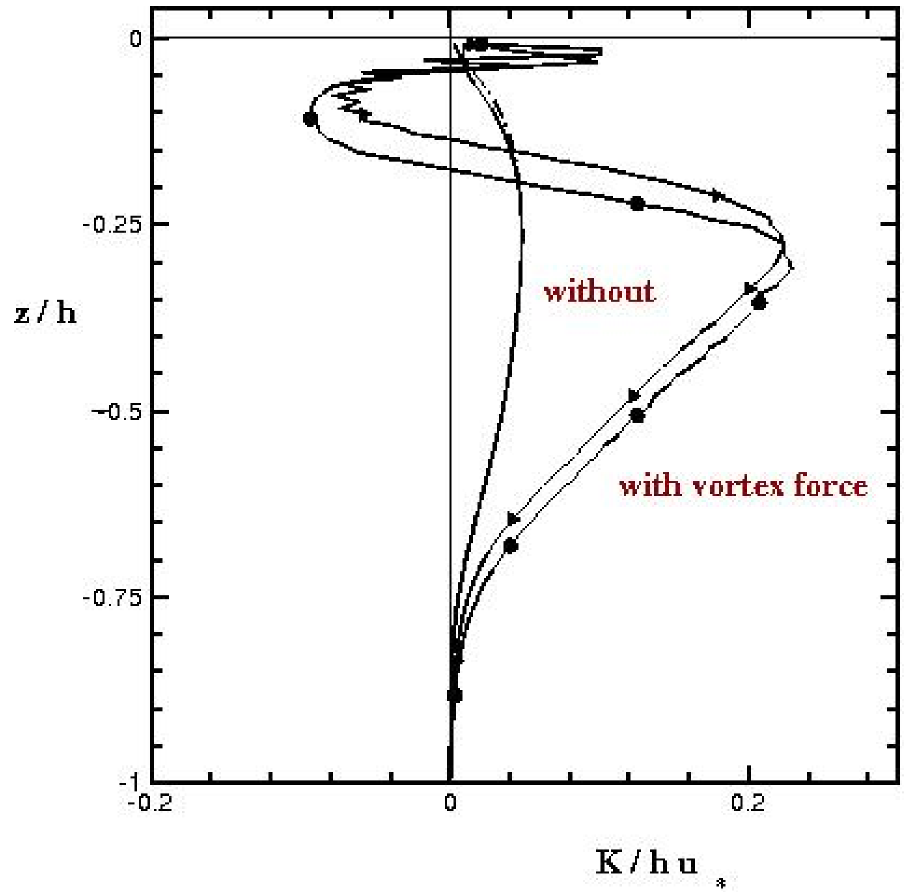

diagnosed eddy viscosity:

$$K \;=\; - < \mathbf{u}'_{\perp} w' > \Big/ \partial_z < \mathbf{u} >_{\perp}$$

⇒ nonlocal, more efficient vertical momentum transport with vortex force.

.

Breaking increases vertical material mixing and turbulent kinetic energy (not shown).

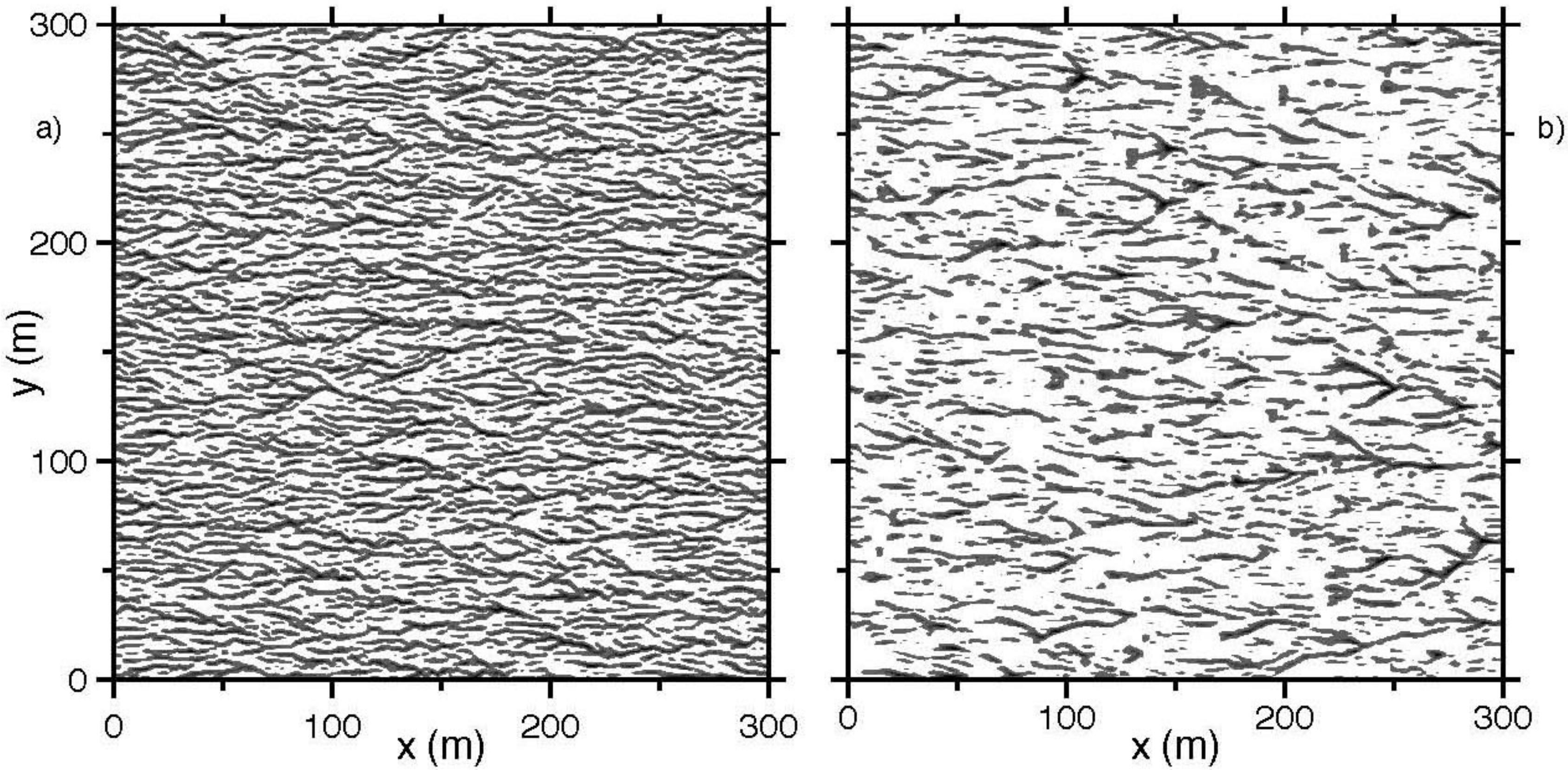

Patterns of strong $w < 0$ near the surface with vortex force: (left) uniform $\boldsymbol{\tau}^{atm}$; (right) breakers with the equivalent mean $\boldsymbol{\tau}$ in a developing sea with $A = c_p/U^{atm} = 0.7$.

.

$\Rightarrow$ breakers & their A dependence influence Langmuir circulations (and mixing rates).

.

. . . these and other wave effects are yet to be incorporated in ROMS' K-Profile Parameterization scheme.

Summary and Prospects

By incorporating WEC in ROMS and adducing surface-wave information ($e.g.,$ from SWAN), we have examined idealized problems for

- coastal and basin-scale infragravity waves and Earth's hum
- unstable littoral currents
- surface turbulent boundary layers

This work is a start on a general framework for exploring other wave-current interaction phenomena, involving fully three-dimensional behaviors, sediment transport, and more realistic configurations.

Bibliography

Sullivan, P.P., J.C. McWilliams, & W.K. Melville, 2007: Surface gravity wave effects in the oceanic boundary layer: Large Eddy Simulation with vortex force and stochastic breakers. *J. Fluid Mech.*

Kanarska, Y., A. Shchepetkin, & J.C. McWilliams, 2007: Algorithm for non-hydrostatic dynamics in the Regional Oceanic Modeling System, *Ocean Modelling*

Uchiyama, Y., & J.C. McWilliiams, 2007: Infragravity waves in the deep ocean: Generation, propagation, and seismic hum excitation. *J. Geophys. Res.*

McWilliams, J.C., J.M. Restrepo, & E.M. Lane, 2004: An asymptotic theory for the interaction of waves and currents in coastal waters. *J. Fluid Mech.*

Lane, E.M., J.M. Restrepo, & J.C. McWilliams, 2007: Wave-current interaction: A comparison of radiation-stress and vortex-force representations. *J. Phys. Ocean.*

Uchiyama, Y., J.C. McWilliams, & J. Restrepo, 2007: Wave-current interaction in the shear instability of a littoral current, in preparation.